Available online at www.sciencedirect.com
ScienceDirect
Journal of Power Sources 161 (2006) 1241–1246
JOURNAL OF POWER SOURCES
www.elsevier.com/locate/jpowsour

Structural and electrochemical characteristics of $LiNi_{0.5-x}Co_{2x}Mn_{1.5-x}O_4$ prepared by spray drying process and post-annealing in O_2

Decheng Li [a], Atsushi Ito [b], Koichi Kobayakawa [b], Hideyuki Noguchi [c], Yuichi Sato [b,*]

[a] *High-Tech Research Center, Kanagawa University, 1-1-40 Suehiromachi, Tsurumi-ku, Yokohama 230-0045, Japan*
[b] *Department of Applied Chemistry, Faculty of Engineering, Kanagawa University, 3-27-1 Rokkakubashi, Kanagawa-ku, Yokohama 221-8686, Japan*
[c] *Department of Applied Chemistry, Saga University, Honjo-1, Saga 840-8502, Japan*

Received 30 March 2006; received in revised form 25 April 2006; accepted 27 April 2006
Available online 12 June 2006

Abstract

$LiNi_{0.5-x}Co_{2x}Mn_{1.5-x}O_4$ ($0 \le 2x \le 0.2$) was prepared by a spray dry process and comparative studies were carried out between the as-prepared series and the series re-annealed in O_2. The cobalt substitution resulted in significant structural and electrochemical variations, such as the transformation of the space group from $P4_332$ to $Fd\bar{3}m$, the increase in the occupancy of cobalt in the tetrahedral sites, and the change in the shape of the charge and discharge profiles, which are related to the progressive oxygen loss. Moreover, an improved rate capability and cyclic performance at high rate was observed for the sample with $2x \ge 0.1$.

Keywords: Li-ion battery; Cathode material; $LiNi_{0.5-x}Co_{2x}Mn_{1.5-x}O_4$; Spray drying and post-annealing; Structural and electrochemical properties

1. Introduction

In the past decade, $LiNi_{0.5}Mn_{1.5}O_4$ has received a great deal of attention as a promising cathode material for lithium secondary batteries. Although it was initially proposed as a 3 V cathode material [1], its 5 V plateau received special attention because it could provide a higher energy density than that at 3 V [2–12], and could be used in electric vehicles (EVs) in the future as well as having the merits of the low cost and toxicity. Because of the difficulty in the preparation by the traditional solid state reaction, $LiNi_{0.5}Mn_{1.5}O_4$ is usually obtained through a solution process, such as sol–gel [2,13], co-precipitation [6,9], emulsion drying [10], and a molten salt method [14] in order to obtain a product with a high purity. The valences of Ni and Mn in the $LiNi_{0.5}Mn_{1.5}O_4$ have been determined to be divalent and tetravalent, respectively. When it is charge in the 5 V voltage region, the Ni^{2+} would be oxidized to Ni^{4+} via Ni^{3+} during lithium-ion extraction from the lattice, while the valence of Mn does not change [7]. $LiNi_{0.5}Mn_{1.5}O_4$ has a cubic structure. However, the cation distribution in the lattice is sensitive to the preparation conditions. $LiNi_{0.5}Mn_{1.5}O_4$ prepared at a high annealing temperature ($\ge$850 °C) adopts a cubic spinel structure with a high symmetry (space group $Fd\bar{3}m$), whereas it adopts a primitive simple cubic structure with a low symmetry (space group $P4_332$) if it was annealed at a low temperature ($\le$700 °C) [15]. Moreover, different phase transformation processes were exhibited during the lithium extraction/insertion from/into the lattice, thereby resulting in different electrochemical behavior [14–17]. In addition to the preparation conditions, the structural and electrochemical properties of the $LiNi_{0.5}Mn_{1.5}O_4$ could also be affected by the substitution of other metal ions such as Al, Mg, Fe, Cu, and Co, and the change in the structural and electrochemical characteristics depends on the dopant [18–22].

In this study, $LiNi_{0.5-x}Co_{2x}Mn_{1.5-x}O_4$ ($0 \le 2x \le 0.2$) was prepared by a spray dry process, and comparative studies were carried out between the as-prepared series and the series re-annealed in O_2. We found that the substitution of cobalt for both Ni and Mn resulted in complicated structural variations, such as the change in the space group, increase in oxygen deficiency and cation mixing, and further affected their electrochemical properties.

* Corresponding author. Tel.: +81 45 481 5661x3885; fax: +81 45 413 9770.
E-mail address: satouy01@kanagawa-u.ac.jp (Y. Sato).

0378-7753/$ – see front matter © 2006 Elsevier B.V. All rights reserved.
doi:10.1016/j.jpowsour.2006.04.120

2. Experimental

Precursors were prepared by a spray drying method, and $LiOH{\cdot}H_2O$, $Ni(NO_3)_2{\cdot}6H_2O$, and $Mn(CH_3COO)_2{\cdot}4H_2O$ were selected as the starting materials. The precisely weighed $Ni(NO_3)_2{\cdot}6H_2O$ and $Mn(CH_3COO)_2{\cdot}4H_2O$ were initially dissolved into a 0.2 M citric solution (Ni:Mn:citric acid is 1:3:4 molar ratio). The resulting solution was pumped into a spray dry instrument (Büchi Mini Spray Dryer B-290). The obtained precursor was pre-heated at 900 °C for 20 h in air. $LiOH{\cdot}H_2O$ was added to the resulting powder (7% molar ratio of lithium is in excess in order to compensate for the possible loss), and the mixture was thoroughly ground, and then pressed into pellets. The pellets were sintered at 700 °C for 24 h in air. Half of them were ground into power and re-treated at 500 °C for 30 h in O_2.

The XRD measurements were carried out using a Rigaku Rint1000 diffractometer equipped with a monochromator and a Cu target tube.

The thermogravimetric analysis (TGA) and differential thermal analysis (DTA) of the precursor were performed in the range from room temperature to 1000 °C at a scan rate of 10 °C min^{-1} using a S II TG–DTA22 (Seiko).

Fourier transform infrared (FT-IR) spectra were recorded by a KBr method using an FT-IR spectrometer.

The charge/discharge tests were carried out using a CR2032 coin-type cell, which consists of a cathode and lithium metal anode separated by a Celgard 2400 porous polypropylene film. The cathode contains a mixture of 20 mg of accurately weighted active materials and 12 mg of teflonized acetylene black (TAB-2) as the conducting binder. The mixture was pressed onto a stainless steel mesh and dried at 130 °C for 4 h. The cells were assembled in a glove box filled with dried argon gas. The electrolyte was 1 M $LiPF_6$ in ethylene carbonate/dimethyl carbonate (EC/DMC, 1:2, v/v).

3. Results and discussion

Fig. 1 shows the XRD patterns of the as-prepared $LiNi_{0.5-x}Co_{2x}Mn_{1.5-x}O_4$ ($0 \le 2x \le 0.2$). All samples have the typical diffraction patterns of a cubic spinel and no impurities were observed in any of the samples.

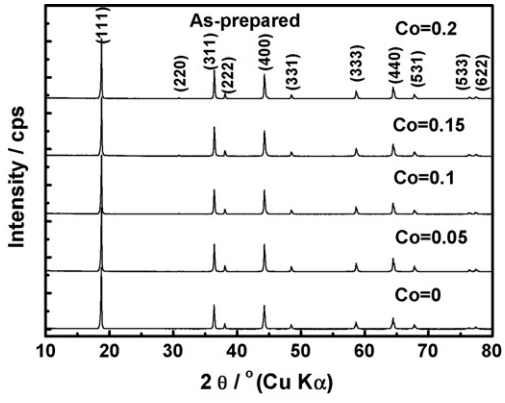

Fig. 1. XRD patterns of the as-prepared $LiNi_{0.5-x}Co_{2x}Mn_{1.5-x}O_4$ ($0 \le 2x \le 0.2$).

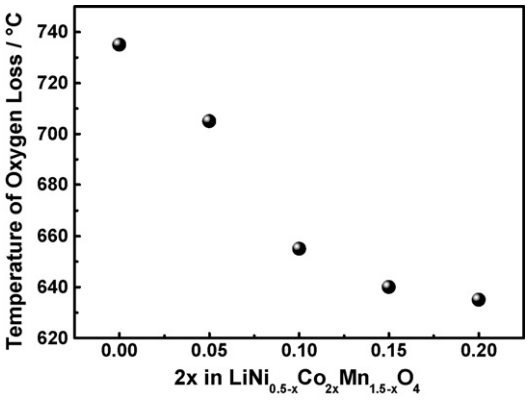

Fig. 2. Starting temperatures of oxygen loss vs. cobalt content for the as-prepared $LiNi_{0.5-x}Co_{2x}Mn_{1.5-x}O_4$ ($0 \le 2x \le 0.2$).

Fig. 2 shows the relationship between the starting temperatures of the oxygen loss and the cobalt content in the as-prepared samples. The starting temperatures of the oxygen loss for all samples were obtained from their TG–DTA profiles. As illustrated in Fig. 2, the starting temperature of the oxygen loss was about 730 °C, quite consistent with the reported value [6]. As the cobalt content increases, the starting temperature of the oxygen loss significantly decreases and the starting temperature of the oxygen loss was about 630 °C for the $LiNi_{0.4}Co_{0.2}Mn_{1.5}O_4$. This result implies that our co-substituted samples should be oxygen-deficient since they were sintered at 700 °C for a long time. Therefore, all samples were re-annealed in O_2 at 500 °C for 30 h in order to compensate for the possible oxygen loss [13].

Fig. 3 shows the enlarged (2 2 0) peaks of the as-prepared $LiNi_{0.5-x}Co_{2x}Mn_{1.5-x}O_4$ and the $LiNi_{0.5-x}Co_{2x}Mn_{1.5-x}O_4$ post-annealed in O_2 ($0 \le 2x \le 0.2$). The intensity of the (2 2 0) peak increases as the cobalt content increases for the samples without the post-treatment in O_2. Since it is sensitive to the dis-

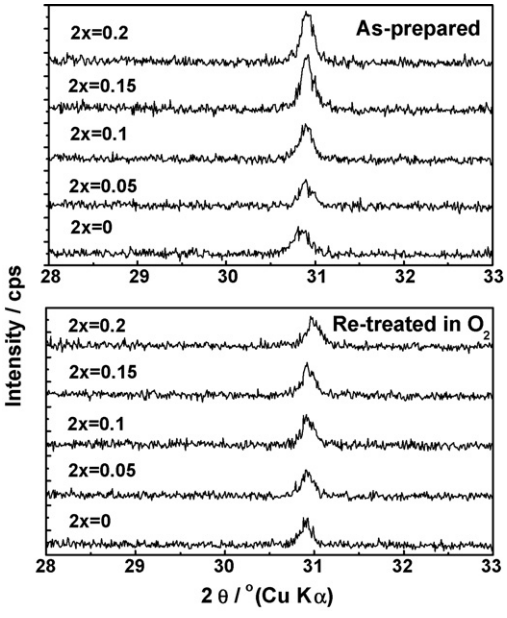

Fig. 3. Enlarged (2 2 0) peaks of the as-prepared $LiNi_{0.5-x}Co_{2x}Mn_{1.5-x}O_4$ and the $LiNi_{0.5-x}Co_{2x}Mn_{1.5-x}O_4$ post-annealed in O_2 ($0 \le 2x \le 0.2$).

tribution of the metal ions in the tetragonal sites, we believe that some cobalt ions occupy the tetrahedral sites with the corresponding displacement of Li to the octahedral sites, because Bruce and co-workers reported that about 25% of the tetrahedral sites were occupied by Co in the spinel $LiCoMnO_4$ [23]. It is interesting to note that the intensity of the (2 2 0) peak significantly decreases compared to that of the untreated sample after being annealed in O_2. These results indicate that the cation mixing is correlated to the oxygen deficiency. Therefore, it is necessary to undergo a structural refinement of those samples.

Before the Rietveld refinements were carried out, the space group of the sample should be determined. Fig. 4 shows the FT-IR results of the $LiNi_{0.5-x}Co_{2x}Mn_{1.5-x}O_4$ ($0 \le 2x \le 0.2$) with and without post-treatment in O_2. There were several absorption bands in the range of 700–400 cm^{-1} for both the untreated $LiNi_{0.5}Mn_{1.5}O_4$ and the re-annealed $LiNi_{0.5}Mn_{1.5}O_4$ although the re-treated sample has well-defined peaks. Although these peaks could not yet be precisely assigned, our results strongly suggested that they have a cubic structure with the $P4_332$ space group, quite consistent with those already reported [6]. However, the number of absorption bands significantly decreased as the cobalt content increased. For the $LiNi_{0.425}Co_{0.15}Mn_{1.425}O_4$ and $LiNi_{0.4}Co_{0.2}Mn_{1.4}O_4$, there are only two broad absorption bands no matter if they were re-treated in O_2, similar to that of the $Li_4Ti_5O_{12}$ whose space group has been determined to be $Fd\bar{3}m$ [16]. These results suggest that the space group of the sample changes from $P4_332$ to $Fd\bar{3}m$ as the cobalt content increases from 0 to 0.2. Therefore, the Rietveld refinements were

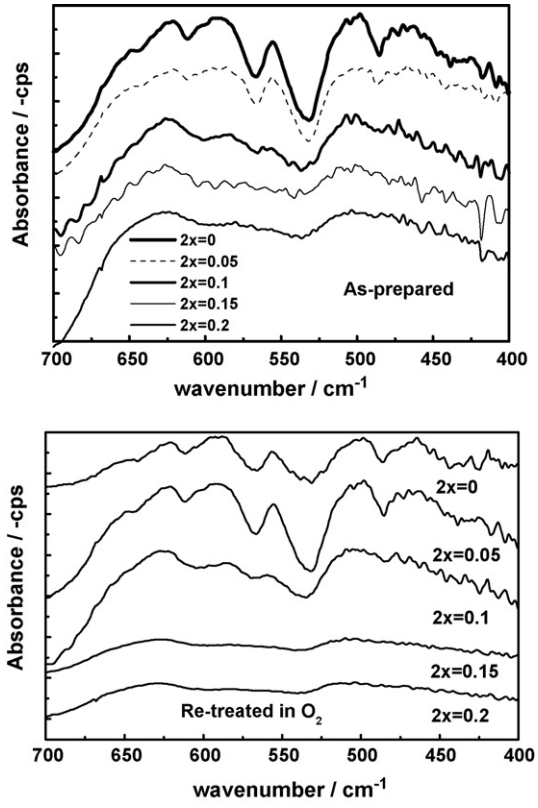

Fig. 4. FT-IR characteristics of the $LiNi_{0.5-x}Co_{2x}Mn_{1.5-x}O_4$ ($0 \le 2x \le 0.2$) with and without post-treatment in O_2.

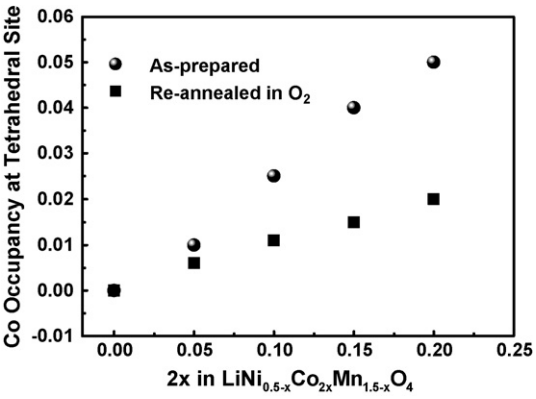

Fig. 5. Cobalt occupancy at tetrahedral sites vs. cobalt content in the $LiNi_{0.5-x}Co_{2x}Mn_{1.5-x}O_4$ ($0 \le 2x \le 0.2$) with and without post-treatment in O_2.

carried out using the space group of $P4_332$ for $LiNi_{0.5}Mn_{1.5}O_4$ and $LiNi_{0.475}Co_{0.05}Mn_{1.475}O_4$ and $Fd\bar{3}m$ for the sample with $2x \ge 0.1$. All the Rietveld refinements have a reliable factor less than 1.5 and some of the refinement results are illustrated in Figs. 5 and 6.

Fig. 5 shows the variation in the cobalt occupancy at the tetrahedral sites as the cobalt content changes in the $LiNi_{0.5-x}Co_{2x}Mn_{1.5-x}O_4$ ($0 \le 2x \le 0.2$) with and without post-treatment in O_2. The occupancy of cobalt at the tetrahedral sites linearly increases as the cobalt content increases for the $LiNi_{0.5-x}Co_{2x}Mn_{1.5-x}O_4$ without the re-treatment in O_2. The occupancies of Co at the tetrahedral site are 2.5 and 5% for the samples with $2x = 0.1$ and 0.2, respectively. The post-annealing treatment in O_2 could significantly decrease the Co occupancy at the tetrahedral sites, and the occupancies are 1% and 2% for the samples with $2x = 0.1$ and 0.2, respectively.

Fig. 6 shows the correlation between the cobalt content and the lattice parameters of the $LiNi_{0.5-x}Co_{2x}Mn_{1.5-x}O_4$ ($0 \le 2x \le 0.2$) with and without post-treatment in O_2. For the samples re-annealed in O_2, the lattice parameter monotonously decreased from 8.168(3) to 8.154(7) Å when $2x$ increased from 0 to 0.2. It is well known that the radii of Co^{3+}, Ni^{2+}, Mn^{3+}, and Mn^{4+} on the octahedral sites are 0.525, 0.690, 0.645, and 0.540 Å [24,25]. Therefore, the substitution of Co^{3+} with the small ionic size for both Ni^{2+} and Mn^{4+} shrinks the lattice volume. For the

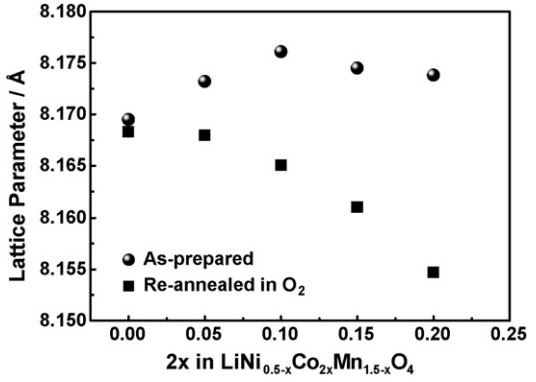

Fig. 6. Lattice parameters vs. cobalt content in the $LiNi_{0.5-x}Co_{2x}Mn_{1.5-x}O_4$ ($0 \le 2x \le 0.2$) with and without post-treatment in O_2.

samples without the post-annealing, the evolution of the lattice parameter as the cobalt content is significantly different from that of the $LiNi_{0.5-x}Co_{2x}Mn_{1.5-x}O_4$ re-annealed in O_2. The lattice parameter initially increased from 8.169(5) to 8.176(1) Å when $2x$ increased from 0 to 0.1, and then decreased to 8.174(5) and 8.173(8) Å for the samples with $2x = 0.15$ and 0.2. We believed that this discrepancy resulted from the difference in the Mn^{3+} content in these samples, given that it had been reported that Mn^{3+} existed in the oxygen-deficient $LiNi_{0.5}Mn_{1.5}O_4$ [2,13]. As mentioned in Fig. 2, the starting temperature of the oxygen loss decreased as the cobalt content increased. This means that the occurrence of the oxygen deficiency becomes easy after the cobalt introduction. Thus, the Mn^{3+} content should increase to compensate for the increase in the oxygen deficiency, and the abnormal evolution of the lattice parameter as the cobalt content should be a balance between the decrease in Ni^{2+} and the increase in Mn^{3+}. Moreover, the influence of the increase in Mn^{3+} is predominant when $x \leq 0.1$ and the influence of the decrease in the Ni^{2+} becomes significant when $x \geq 0.1$.

Fig. 7 shows the initial charge and discharge curves of the as-prepared $LiNi_{0.5-x}Co_{2x}Mn_{1.5-x}O_4$ ($0 \leq 2x \leq 0.2$) operated at a current density of 0.2 mA cm^{-2} (20 mA g^{-1}) in the voltage range of 3–4.9 V. A small plateau near 4 V, which corresponds to the Mn^{3+}/Mn^{4+} redox, was observed in the initial charge and discharge curves of the $LiNi_{0.5}Mn_{1.5}O_4$. The capacity of this plateau gradually increases as the cobalt content increases. This result strongly suggests that the Mn^{3+} content increases with the increase in the cobalt content. On the other hand, both the charge and discharge capacities in the high-voltage plateau gradually decrease as the cobalt content increases, which should originate from the decrease in the Ni^{2+} content. These results also confirmed our judgment regarding the reason for the abnormal change in the lattice parameter as already mentioned. Alcántara et al. [21] also observed the slight increase in the cell parameter of the $LiNi_{0.4}Co_{0.2}Mn_{1.4}O_4$ and ascribed it to the decrease in the average oxidation state of manganese caused by the progressive loss of oxygen. Moreover, the charge and discharge profiles gradually change from the flat two-step shape for the $LiNi_{0.5}Mn_{1.5}O_4$ to the sloping two-step shape for the $LiNi_{0.4}Co_{0.2}Mn_{1.4}O_4$. It has been reported that the binding energy of the Li atom to the host was strongly affected by its local environment (the nearest neighbor, i.e., the anion) [3] and the range of the binding energies of the Li atom resulted in a sloping voltage profile for the $Mo_xSe_zS_{8-z}$ with the spinel structure [26]. The variation in the charge/discharge curve for our samples implies that the substitution of cobalt for Ni and Mn results in a significant change in the nearest neighbor oxygen environment, which should be related to the progressive loss of oxygen.

The charge and discharge curves of the $LiNi_{0.5-x}Co_{2x}Mn_{1.5-x}O_4$ ($0 \leq 2x \leq 0.2$) re-treated in O_2 are shown in Fig. 8. The cells were operated at a current density of 0.2 mA cm^{-2} (20 mA g^{-1}) in the voltage range of 3–4.9 V. The 4 V plateau in the charge and discharge curves was significantly depressed for all samples after they were re-annealed in O_2, and the discharge capacity of the $LiNi_{0.4}Co_{0.2}Mn_{1.4}O_4$ in the 4 V plateau is about 5 mA h g^{-1}, lower than that of the as-prepared $LiNi_{0.4}Co_{0.2}Mn_{1.4}O_4$ (about 12 mA h g^{-1}). Moreover, both the charge and discharge capacities (the sum of the high-voltage capacity and the 4 V voltage capacity) decreased as the cobalt content increased, which should be attributed to the decrease in the Ni^{2+} content (the plateau of the Co^{3+}/Co^{4+} redox should occur at 5.1 V), quite consistent with the monotonous decrease in the lattice parameter. The voltage profile of the $LiNi_{0.4}Co_{0.2}Mn_{1.4}O_4$ reverses to the flat two-step type after it was annealed in O_2. The voltages for these two plateaus are 4.75 and 4.6 V, and the difference between them is 0.15 V, higher than that of the $LiNi_{0.5}Mn_{1.5}O_4$ and the $LiNi_{0.475}Co_{0.05}Mn_{1.475}O_4$ (about 0.03 V). Further work is necessary to characterize the structural change during the charge and discharge cycling.

The oxygen content of the $LiNi_{0.5-x}Co_{2x}Mn_{1.5-x}O_4$ ($0 \leq 2x \leq 0.2$) with and without the re-treatment in O_2 was roughly estimated by measuring the capacity at 4 V plateau and calculating the average valence of Mn, assuming that the elemental ratio among Li, Ni, Co, Mn is the same with its nominal chemical composition, and the valences for the Ni and Co are divalent and trivalent. Moreover, the theoretical capacity for Mn^{3+}/Mn^{4+} redox per molar in the $LiNi_{0.5-x}Co_{2x}Mn_{1.5-x}O_4$ was assumed to be 148 mA h g^{-1} in our calculation. The calculated results are shown in Fig. 9. As illustrated in Fig. 9, the oxygen deficiency became severely as cobalt content increased

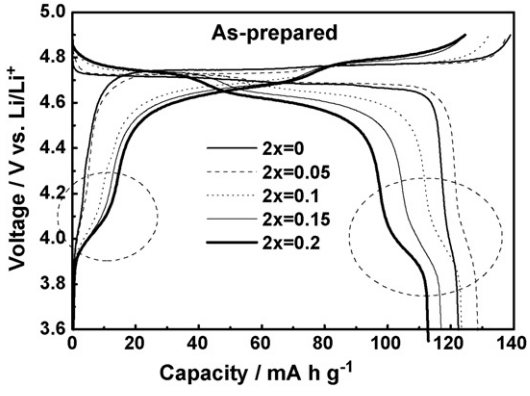

Fig. 7. Initial charge and discharge curves of the as-prepared $LiNi_{0.5-x}Co_{2x}Mn_{1.5-x}O_4$ ($0 \leq 2x \leq 0.2$) operated in the voltage range of 3–4.9 V.

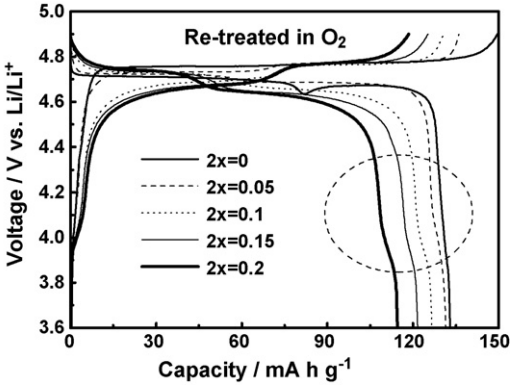

Fig. 8. Initial charge and discharge curves of the $LiNi_{0.5-x}Co_{2x}Mn_{1.5-x}O_4$ ($0 \leq 2x \leq 0.2$) re-treated in O_2 operated in the voltage range of 3–4.9 V.

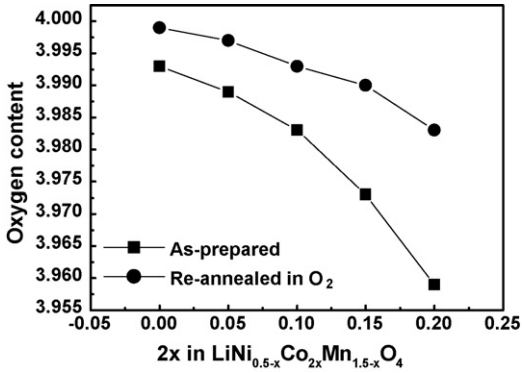

Fig. 9. Oxygen content of the $LiNi_{0.5-x}Co_{2x}Mn_{1.5-x}O_4$ ($0 \le 2x \le 0.2$) with and without re-treatment in O_2.

for the as-prepared samples. The oxygen contents for the sample with $2x = 0$, 0.05, 0.1, 0.15, and 0.2 are 3.993, 3.989, 3.989, 3.972, and 3.959, respectively. After being annealed in O_2, most of the lost oxygen was recovered. The oxygen contents are 3.992, 3.990, and 3.983 for $2x = 0.1$, 0.15, and 0.2.

The rate capabilities of the $LiNi_{0.5-x}Co_{2x}Mn_{1.5-x}O_4$ ($0 \le 2x \le 0.2$) with and without the re-treatment in O_2 are given in Fig. 10. All cells were initially operated for one cycle at a current density of 0.2 mA cm^{-2} (20 mA g^{-1}). From the second cycle on, the charge current density was kept at the constant current density of 0.2 mA cm^{-2}, while the discharge capacities changed from 0.2 (about 0.15 C) to 0.4, 0.8, 1.6, 3.2, and 4.8 mA cm^{-2} (about 3.5 C) in subsequent cycles. The discharge capacity of the as-prepared $LiNi_{0.5}Mn_{1.5}O_4$ is about 129 mA h g^{-1} at 0.15 C and decreases to about 113 mA h g^{-1} (about 87% of its initial discharge capacity) when the discharge rate increases to 3.5 C. All the as-prepared co-substituted samples have excellent rate performances. The discharge capacities for the samples with $2x = 0.05$, 0.1, 0.15, and 0.2 are 131, 126, 121, and 116 mA h g^{-1} at 0.15 C and 121, 117, 112, and 107 mA h g^{-1} at 3.5 C, respectively. More than 92% of their initial discharge capacities are available when the discharge rate increases to 3.5 C. For the samples re-treated in O_2, the discharge capacity of the $LiNi_{0.5}Mn_{1.5}O_4$ is about 136 mA h g^{-1} at 0.15 C and decreased to about 125 mA h g^{-1} (about 92% of its initial discharge capacity) when the discharge rate increased to 3.5 C, better than that of the as-prepared $LiNi_{0.5}Mn_{1.5}O_4$. The discharge capacities of the $LiNi_{0.475}Co_{0.05}Mn_{1.475}O_4$ at 0.15 C and 3.5 C are 133 and 119 mA h g^{-1}, respectively. Its capacity retention is about 89%, lower than that of the $LiNi_{0.5}Mn_{1.5}O_4$, which should be related to the increased cation mixing degree. The discharge capacities for the samples with $2x = 0.1$, 0.15, and 0.2 are 128, 123, and 116 mA h g^{-1} at 0.15 and 118, 114, and 107 mA h g^{-1} at 3.5 C, respectively. The capacity retention is greater than 92% for all of them. We are not very sure if it is appropriate to make a direct comparison between the samples with $2x < 0.1$ and the samples with $2x \ge 0.1$, given that they have

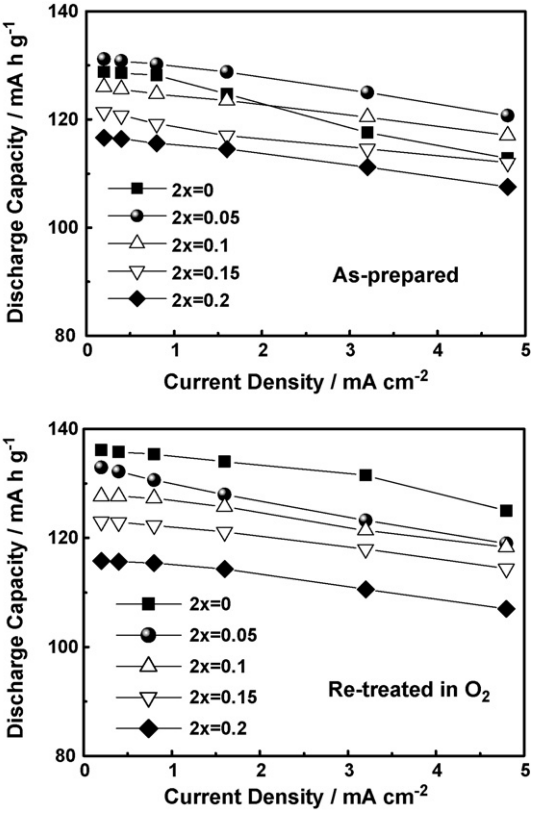

Fig. 10. Rate capabilities of the $LiNi_{0.5-x}Co_{2x}Mn_{1.5-x}O_4$ ($0 \le 2x \le 0.2$) with and without re-treatment in O_2.

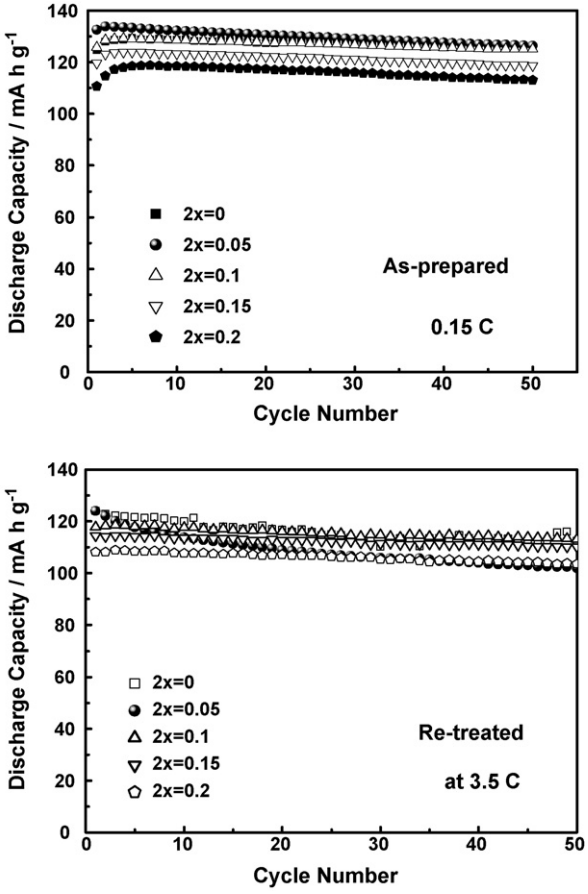

Fig. 11. Cyclic performance of the $LiNi_{0.5-x}Co_{2x}Mn_{1.5-x}O_4$ ($0 \le 2x \le 0.2$) operated in the voltage range of 3–4.9 V at different *C* rates.

different space groups. In both cases, however, the rate properties of the samples with the space group of $Fd\bar{3}m$ seem to be better than those of the samples with a space group of $P4_332$ in spite of their relatively high cation mixing degree. It has been reported that the cobalt substitution for both Ni and Mn in the layered $LiNi_{0.5}Mn_{0.5}O_2$, where the valences for Ni and Mn are the same as those in the $LiNi_{0.5}Mn_{1.5}O_4$, could effectively lower the area specific impedance (ASI) of the layered $LiNi_{0.5}Mn_{0.5}O_2$ and enhance its electronic conductivity [27]. More study is necessary to clarify if the improved rate capability originated from the structural change or the electronic conductivity.

Fig. 11 shows the cyclic performances of the $LiNi_{0.5-x}Co_{2x}Mn_{1.5-x}O_4$ $(0 \leq 2x \leq 0.2)$ operated at different C rates in the voltage range of 3–4.9 V. The as-prepared $LiNi_{0.5-x}Co_{2x}Mn_{1.5-x}O_4$ exhibit good cyclic performances when they were operated at a rate of 0.15 C. The reversible capacities after 50 cycles are 126, 126, 125, 119, and 113 for the samples with $2x = 0$, 0.05, 0.1, 0.15, and 0.2. When the $LiNi_{0.5-x}Co_{2x}Mn_{1.5-x}O_4$ re-annealed in O_2 was operated at 3.5 C, capacity fading was observed for the $LiNi_{0.5}Mn_{1.5}O_4$ and $LiNi_{0.475}Co_{0.05}Mn_{1.475}O_4$. The reversible capacities after 50 cycles are 112 and 102 mA h g^{-1}, respectively. These are about 91 and 82% corresponding to their initial discharge capacities. No obvious capacity fading was observed for the samples with $2x \geq 0.1$. The reversible capacities after 50 cycles are 113, 110, and 104 mA h g^{-1} for the samples with $2x = 0.1$, 0.15, and 0.2, respectively, which are about 96% of their initial discharge capacities.

4. Conclusion

The substitution of cobalt for Ni and Mn in the $LiNi_{0.5}Mn_{1.5}O_4$ resulted in significant structural and electrochemical variations, such as the transformation of the space group from $P4_332$ to $Fd\bar{3}m$, the increase in the occupancy of cobalt at the tetrahedral sites, and the change in the shape of the charge and discharge profiles. We believe that all these variations are related to the progressive oxygen loss due to the decrease in the starting temperature of the oxygen loss. Although the cobalt substitution generally decreases the initial discharge capacity due to the decrease in the Ni content, an improved rate capability and cyclic performance at high rate was observed for the sample with $2x \geq 0.1$ compared to those of the $LiNi_{0.5}Mn_{1.5}O_4$.

Acknowledgement

This work was financially supported by the High-Tech Research Center Project for Private University: matching fund subsidy from the Ministry of Education, Culture, Sports, Science and Technology (MEXT) from 2001 to 2005.

References

[1] K. Amine, H. Tukamoto, H. Yasuda, Y. Fujita, J. Electrochem. Soc. 143 (1996) 1607.
[2] Q. Zhong, A. Bonakdarpour, M. Zhang, Y. Gao, J. Dahn, J. Electrochem. Soc. 144 (1997) 205.
[3] Y. Gao, K. Myrtle, M. Zhang, J.N. Reimer, J.R. Dahn, Phys. Rev. B 54 (1996) 16670.
[4] T. Zheng, J.R. Dahn, Phys. Rev. B 56 (1997) 3801.
[5] T. Ohzuku, S. Takeda, M. Iwanaga, J. Power Sources 81–82 (1999) 90.
[6] T. Ohzuku, K. Ariyoshi, S. Yamamoto, Y. Makimura, Chem. Lett. (2001) 1270.
[7] Y. Terada, K. Yasaka, F. Nishikawa, T. Konishi, M. Yoshio, I. Nakai, J. Solid State Chem. 156 (2001) 286.
[8] R. Alcándara, M. Jaraba, P. Lavera, J. Tirado, Electrochim. Acta 47 (2002) 1829.
[9] Y.S. Lee, Y.K. Sun, S. Ota, T. Miyashita, M. Yoshio, Electrochem. Commun. 4 (2002) 989.
[10] S.T. Myung, S. Komaba, N. Kumakai, H. Yashiro, H.T. Chung, T.H. Cho, Electrochim. Acta 47 (2002) 2543.
[11] T. Ohzuku, K. Ariyoshi, S. Yamamoto, J. Ceram. Soc. Jpn. 110 (2002) 501.
[12] K. Dokko, M. Mohamedi, N. Anzue, T. Itoh, I. Uchida, J. Mater. Chem. 12 (2002) 3688.
[13] Y. Idemoto, H. Narai, N. Koura, J. Power Sources 119–121 (2003) 125.
[14] J.H. Kim, S.T. Myung, C.S. Yoon, S.G. Kang, Y.K. Sun, Chem. Mater. 16 (2004) 906.
[15] J.H. Kim, C.S. Yoon, S.T. Myung, J. Prakashi, Y.K. Sun, Electrochem. Solid-State Lett. 7 (2004) A216.
[16] K. Ariyoshi, Y. Iwakoshi, N. Nakayama, T. Ohzuku, J. Electrochem. Soc. 151 (2004) A296.
[17] Y. Idemoto, H. Sekine, K. Ui, N. Koura, Solid State Ionics 176 (2005) 299.
[18] Y. Ein-Eli, J.T. Vaughey, M.M. Thackeray, S. Mukerjee, X.Q. Yang, J. McBreen, J. Electrochem. Soc. 146 (1999) 908.
[19] G.T.K. Fey, C.Z. Lu, T.P. Kumar, J. Power Sources 115 (2003) 332.
[20] R. Alcántara, M. Jaraba, P. Lavela, J.L. Tirado, E. Zhecheva, R. Stoyanova, Chem. Mater. 16 (2004) 1573.
[21] R. Alcántara, M. Jaraba, P. Lavela, J.L. Tirado, J. Electrochem. Soc. 151 (2004) A53.
[22] R. Alcántara, M. Jaraba, P. Lavela, J.M. Lloris, C.P. Vicente, J.L. Tirado, J. Electrochem. Soc. 152 (2005) A13.
[23] A.D. Robertson, A.R. Armstrong, P.G. Bruce, J. Power Sources 97–98 (2001) 332.
[24] Y. Shao-Horn, R.L. Middaugh, Solid State Ionics 139 (2001) 13.
[25] R.D. Shannon, Acta Crystallogr., Sect. A 32 (1976) 751.
[26] L.S. Selwyn, W.R. McKinnon, J.R. Dahn, Y. LePage, Phys. Rev. B 33 (1986) 6405.
[27] S.-H. Kang, J. Kim, M.E. Stoll, D. Abraham, Y.K. Sun, K. Amine, J. Power Sources 112 (2002) 41.